Dispersions of Attractive Semiflexible Fiberlike Colloidal Particles from Bacterial Cellulose Microfibrils

Anke Kuijk,*[†] Remco Koppert,[†] Peter Versluis,[†] Gerard van Dalen,[†] Caroline Remijn,[†] Johan Hazekamp,[†] Jaap Nijsse,[†] and Krassimir P. Velikov*[†,‡]

[†]Unilever R&D Vlaardingen, Olivier van Noortlaan 120, 3133 AT Vlaardingen, The Netherlands
[‡]Soft Condensed Matter, Debye Institute for NanoMaterials Science, Utrecht University, Princetonplein 5, 3584 CC Utrecht, The Netherlands

S *Supporting Information*

ABSTRACT: We prepared dispersions from bacterial cellulose microfibrils (CMF) of a commercial Nata de Coco source. We used an ultra-high-energy mechanical deagglomeration process that is able to disperse the CMFs from the pellicle in which they are organized in an irregular network. Because of the strong attractions between the CMFs, the dispersion remained highly heterogeneous, consisting of fiber bundles, flocs, and voids spanning tens to hundreds of micrometers depending on concentration. The size of these flocs increased with CMF concentration, the size of the bundles stayed constant, and the size of the voids decreased. The observed percolation threshold in MFC dispersions is lower than the theoretical prediction, which is accounted for by the attractive interactions in the system. Because bacterial cellulose is chemically very pure, it can be used to study the interaction of attractive and highly shape-anisotropic, semiflexible fiberlike colloidal particles.
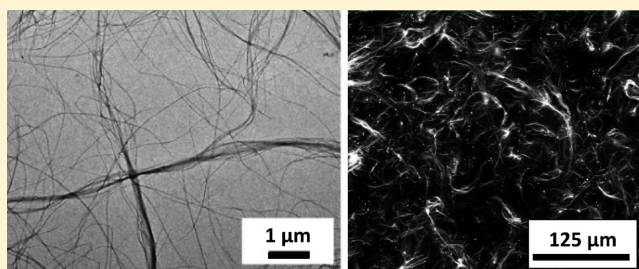
INTRODUCTION

Colloidal dispersions of shape anisotropic (fiberlike) particles of high aspect ratios show many interesting phenomena. Their liquid-crystalline phase behavior, for example, has received much attention in research over the last few decades.[1,2] But besides these more or less ordered liquid-crystalline states, shape-anisotropic colloidal particles can also form disordered networks with an interesting rheological response. The mechanical response of the cytoskeleton, for instance, is produced by networks of actin filaments and microtubules.[3,4] Another system that has received much attention in the literature is that of cellulose microfibrils (CMFs), which can be obtained from different sources, such as wood, plants, and bacteria. In this letter, we used bacterial cellulose (BC). BC consists of long CMFs and finds applications in food,[5] medical,[6,7] and technical fields.[8] In contrast to other well-known types of cellulose, such as cellulose from wood sources, BC is chemically very pure. It is not associated with any hemicelluloses or lignin. Furthermore, it has no functional groups other than hydroxyl groups (i.e., it does not have residual groups—those generated during lignin removal and bleaching in wood-pulp-derived CMF).[6,7] Importantly, the microfibrils in bacterial cellulose are not present in the form of fibers, as in the case of wood pulp cellulose, but as a 3D aggregated network of significantly smaller ribbonlike microfibrils. Hence, the structural history of the system during the deagglomeration process will be very different. The hydroxyl groups on the surface of the microfibrils allow for strong interfibrillar hydrogen bonding and van der Waals interactions, which are on the order of $10kT/\mu$m at a distance of 10 nm for this system (SI). These attractive interactions, in combination with the long aspect ratio of the particles, cause the formation of extended networks when the microfibrils are dispersed in water, defining a unique colloidal system. Because of their high purity, we intend to use fiberlike particles from BC to study the behavior of colloidal dispersions of highly shape-anisotropic, semiflexible fiberlike particles with attractive interactions.

Although BC has been widely studied and explored for various applications,[9] the research has been mainly focused on the mechanism of formation of BC, with the aim of controlling the production and characterization of the pellicles.[10,11] Less attention has been paid to CMF dispersions in relation to deagglomeration approaches to the formation and characterization of the resulting dispersions.[12,13] In addition, most studies on CMF dispersions have been done on cellulose whiskers[14] (i.e., partially hydrolyzed) and on cellulose microfibrils of which the surface was modified as a result of the bleaching, oxidation, or hydrolysis processes in the production.[15] In this letter, we describe the preparation of colloidal dispersions of fiberlike CMF particles from a commercially available source and study the dispersion and particle properties. The fiberlike colloidal particles were prepared by

the mechanical dispersion of CMFs from Nata de Coco sources. To break the bonds that hold the MFCs in the pellicle together, we applied a high-pressure deagglomeration procedure using much higher pressures than generally described in the literature.[16]

MATERIALS AND METHODS

Eight cups of Nata de Coco pellicle cubes (Sari Kelapa Murni, PT Menacoco Sari) were cut using a hand blender (Braun 4185545) and washed with demineralized water. Each washing step consisted of rinsing the dispersion over a vacuum filter and redispersing the residue in 1.5 L of fresh water using a hand blender. After seven washing steps, the filtered liquid and the residue were both colorless. At this point, we assumed that all water-soluble sugars and other additives (i.e., water-soluble colorants, citric acid, and sodium benzoate) were removed from the dispersion. The washed dispersions were processed using a microfluidizer (Microfluidizer M 110S (MF), Microfluidics) at a pressure of 1200 bar. The dispersion was passed through a Z chamber (diameter 87 μm) several times (N). The volume fraction (φ) of the thus-obtained dispersions was determined by drying approximately 20 g of dispersion in a vacuum oven at 40 mbar and 40 °C for 3 days. Here, we take the density of cellulose as 1.5 g/mL.[17]

The microstructure of the MFC dispersions was studied using transmission electron microscopy (TEM), scanning electron microscopy (SEM), and confocal laser scanning microscopy (CLSM). TEM was performed on a Tecnai 20 system from the FEI Company. To determine the diameter of the microfibrils, the samples were negatively stained using phosphotungstic acid. SEM was performed on a Jeol 6340 field-emission electron microscope equipped with an Oxford CT 1500 HF cryosystem. Samples were plunge-frozen in melting ethane. The cryo-fixed samples were cryo-planed and sputter-coated with gold or palladium to obtain a better contrast.

For fluorescent staining, 1 drop of 0.5% Congo red solution in water was added to 1 mL of dispersion. The images were taken using a Leica TCS-SP5 confocal microscope. The confocal images were analyzed using ImageJ. For the autocorrelation, the "radially averaged autocorrelation" macro was used, as can be downloaded from http://imagejdocu.tudor.lu/. To determine floc and void sizes, a morphological sieve method[18] was used on images of 775 × 775 μm^2. The method was directly applied to the gray-level image without the segmentation (thresholding) or separation of objects. Only a median filter and percentile stretching (95/5%) was used as preprocessing, before computing the granulometry.

The rheology measurements were performed on a stress-controlled rheometer (AR 2000, TA Instruments) using a plate–plate geometry (plate diameter 4 cm, gap 1 mm). Sand-blasted metal plates were used to prevent slipping. Frequency sweeps were performed in the range of 0.01–100 Hz at a strain of 0.1%. Shear viscosity was monitored by increasing the shear rate from 0.1 to 500 s^{-1} in 2 min. All measurements were performed at 20 °C.

RESULTS AND DISCUSSION

In our starting material—the Nata de Coco pellicle cubes—the CMFs were arranged in an irregular network such as shown in the SEM images of Figure 1a,b. After deagglomeration at high pressure, the combined effect of the high shear rate (~10^7 s^{-1}) in the microfluidizer, large wall impact, and rapid expansion tore the network into smaller pieces (Figure 1c–f). The resulting particles were flexible microfibrils with an average length (L) that was too long ($L > 10$ μm) to be measured accurately by electron microscopy and an average width of 60 nm. The elementary fibrils that are the building blocks of the ribbonlike microfibrils had a width of about 3 nm, as clearly visible in a negatively stained TEM image (Figure 2b). This value corresponds well to the diameter found by Kose et al., who studied BC dispersed using aqueous counter collision.[19]
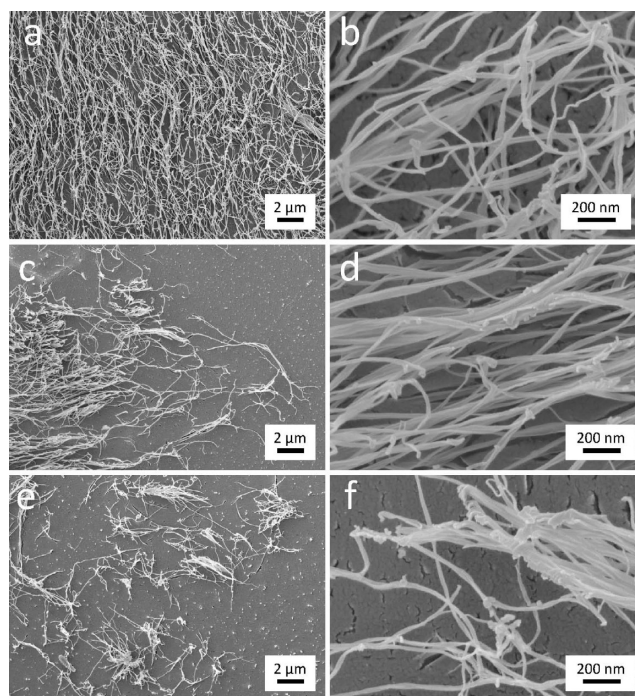
Figure 1. SEM micrographs of fiberlike particles from cellulose microfibrils from BC. (a, b) Untreated pellicle. (c, d) Dispersion using a mechanical blender. (e, f) Homogenized 10 times ($N = 10$). The average length of the cellulose fibrils decreased, and their diameter was not affected by the deagglomeration process.
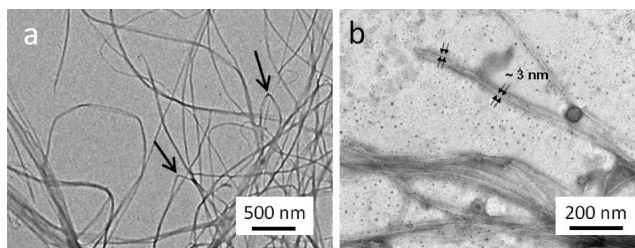
Figure 2. TEM micrographs of BC microfibrils ($N = 1$) showing their dimensions and flexibility. (a) The arrows point out sharp kinks in the fibers after deagglomeration. (b) The diameter of the smallest elementary fibril is clearly visible on the negatively stained image.

The SEM micrographs clearly display the attractive nature of the microfibrils: single fibrils were not found and microfibrils always appeared to be connected to neighboring fibrils, even after multiple deagglomeration passes. Hydrogen bonding and van der Waals attractions between the cellulose microfibrils also caused bundling, which is known to appear in other shear-induced aggregated systems of (attractive) rodlike particles as well.[20] Multiple deagglomeration passes in the preparation procedure resulted in the appearance of shorter microfibrils (Figure 1e), although this effect was not quantified. The formation of shorter microfibrils is probably the result of breakage of the long microfibrils, which is possible due to the high crystallinity of the BC (typically >60%).[21]

In TEM micrographs, we observed an interesting feature of the fiberlike particles, namely, that they showed kinks with very sharp angles when they had been homogenized (arrows in Figure 2a). During the deagglomeration process, the microfibrils were subjected to both expansion under very high pressure (1200 bar) and impact collision on the walls in the Z-

shaped interaction chamber. Both actions can lead to (transient) deagglomeration and breakage of the microfibrils to shorter ones. The exact mechanism of fiber shortening is not established, but TEM micrographs suggest that breakage occurs in the crystalline areas of the MFC, where sharp kinks are observed. The co-occurrence of kinks and bends might be attributed to the presence of alternating areas of amorphous and crystalline cellulose in the microfibrils.

On a somewhat larger length scale, the microstructure of the CMF dispersions was imaged using CLSM.

An impression of what the real-space network of cellulose microfibrils looks like is shown in Figure 3. At all
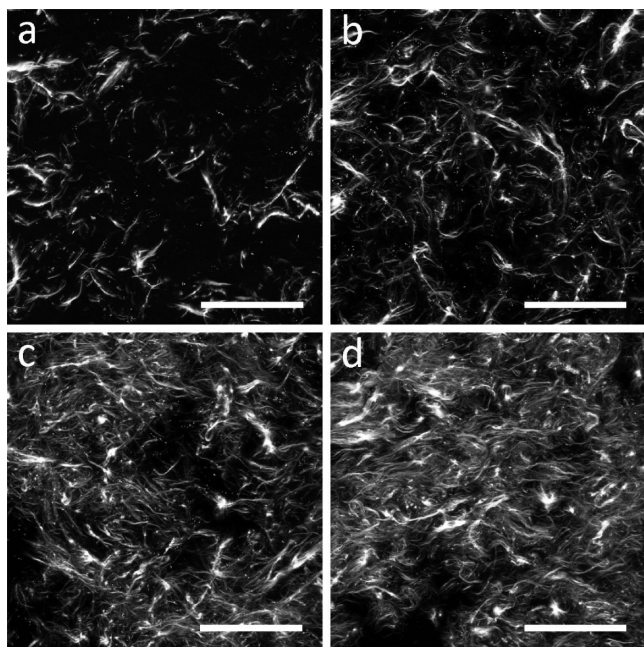
Figure 3. CLSM images of CMF dispersions ($N = 1$) from BC. $\phi =$ (a) 0.07, (b) 0.33, (c) 0.6, and (d) 0.87%. Scale bars indicate 125 μm. These are projections of 10 images taken in 20 μm of z space.

concentrations, the microfibrils formed heterogeneous bundles as a result of the attractive interaction between the microfibrils. Although the network became denser at higher concentrations, large void areas spanning tens to hundreds of micrometers were still visible in the highest-density sample (Figure 3d and SI). The dispersions thus consisted of flocs and bundles of CMFs, which were formed by the attractive interactions caused by hydrogen bonding and van der Waals attractions between them. The attractive nature of the fibrils also caused them to aggregate at lower concentrations so that stable dispersions of single microfibrils were never achieved upon dilution. The typical diameter of the MFC bundles was estimated by calculating the autocorrelation of the image and fitting a single exponential through the beginning of the curve. This resulted in a value of around 15 μm for all of the concentrations shown in Figure 3. Furthermore, we used a morphological sieve method to analyze the size of the bundles and flocs and voids in the micrographs. Figure 4 shows that the distribution of the features found is log normal, which was also found for CMF from wood sources. The median of the distributions was constant for increasing microfibril concentration, and the span of the distribution increased. This means that larger flocs started occurring at higher MFC concentration whereas the
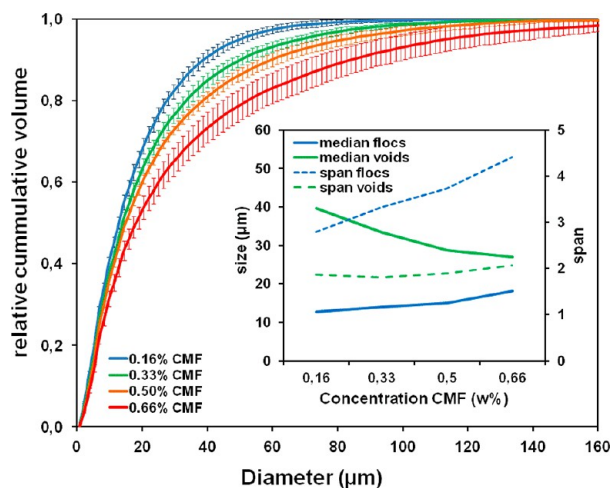
Figure 4. Relative cumulative distribution of floc sizes for different CMF concentrations. The inset shows the median and span values for the log-normal distributions of floc size and void size.

bundle size remained constant at about 15 μm (more details in the SI). Furthermore, the voids decreased with higher microfibril concentration, meaning that the network became more homogeneous.

The constant bundle size might be explained by the accumulation of charges. Typically, a zeta potential of around 50 mV is needed for good colloidal stability. Bacterial cellulose has a zeta potential of only −7 mV;[22] therefore, the microfibrils aggregate. The classical picture for the formation of inorganic colloids dictates that primary particles aggregate until the charge of the aggregate is so high that a collision of two such aggregates does not lead to a larger aggregate. We think a similar process applies to the microfibrils; at a bundle size of about 15 μm the total charge of the bundles is large enough to counteract the short-range attractive van der Waals forces (which are on the order of $10kT/\mu$m at a distance of 10 nm for this system) so that bundle growth is stopped.

Depending on their concentration, dispersions of CMF formed a self-supporting network that spanned the entire solution at higher concentrations and a collapsed gel at lower concentrations (Figure 5). When a self-supporting network was formed, no sedimentation of microfibrils was observed, even though the density of the cellulose microfibrils is higher than that of the solvent (1.5 g/mL compared to 1.0 g/mL). The self-supporting colloidal gels result from a balance between the gravitational stress (σ_g) and the yield stress (σ_y), which is

Figure 5. CMF dispersions ($N = 1$) that form a collapsed gel at a concentration of 0.02% and a space-filling network at a concentration of 0.25% for a sample height of 4.0 cm.

determined by its resistance to fluid flow and its elastic and plastic properties. Factors that influence whether a gel collapses include the volume fraction and height of the sample.[23] At small sample heights, the influence of gravity is small and sedimentation becomes an indication of the percolation threshold. For wood-derived CMF, the threshold for entanglement was found to be $\varphi \geq a/L$, where a is the radius of the fibrils and L is their length.[24] From our TEM measurements, we know that $2a \approx 60$ nm and L is tens of micrometers. The threshold for percolation is then estimated at $\varphi \geq 0.1\%$. Sedimentation experiments, however, showed no collapse of the network for concentrations as low as 0.01% (at 1 cm sample height, see the SI). This lower value for the percolation threshold might be explained by the attractive interactions that are present in the system and that are known to lower the percolation threshold.[25] Additionally, polydispersity in the length of the microfibrils influences the percolation threshold.[26]

The viscoelastic properties of the percolating networks formed by cellulose fibrils were studied using rheology. The results for modules and viscosity measurements are shown in Figure 6. Figure 6 shows that the G' of the CMF networks is
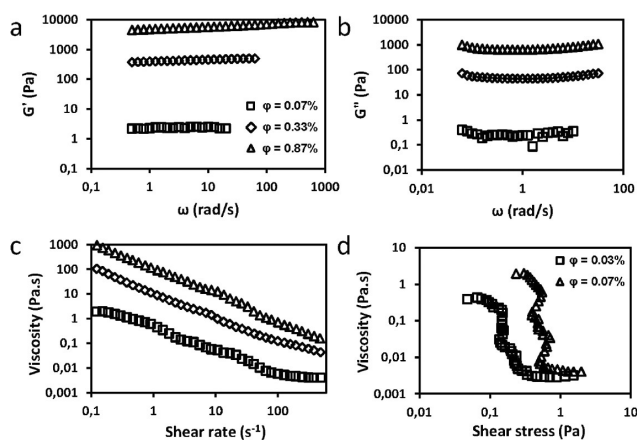

Figure 6. Rheology of CMF dispersions from BC ($N = 1$). (a, b) Frequency dependence of the storage modulus (G') and the loss modulus (G''). (c) Viscosity as a function of shear rate showing shear-thinning behavior. (d) Viscosity as a function of shear stress.

larger than G'' at all concentrations, which is an indication of gel-like behavior. Furthermore, the loss tangent ($\tan \delta$) values, which measure the ratio of the loss modulus to the elastic modulus (G''/G'), were 0.15 ± 0.02 for all concentrations. This also indicates that the suspensions are predominantly elastic. The fact that G' does not depend on frequency confirms the gel-like behavior of the CMF dispersions. Viscosities were measured as a function of shear rate (Figure 6c). All samples showed a strong decrease in viscosity for higher shear rates, which means that the samples were shear thinning. Probably the shear reduces the connections between flocs, which made the dispersion flow more easily.[27] Furthermore, the viscosity of the samples increased with increasing fiber concentration and increasing network density, as expected. Similar rheological results were reported for wood cellulose.[28] Finally, Figure 6d shows clear signs of shear banding, resulting from areas that are more dense and less dense in MFC because multiple viscosities were measured for one value of the shear stress.

The storage and loss modulus of the gels that were formed by the microfibrils depended weakly on the preparation procedure of the dispersion. When the dispersions had passed the homogenizer multiple times, G' and G'' decreased slightly (Figure 7). This was probably caused by the fact that both the
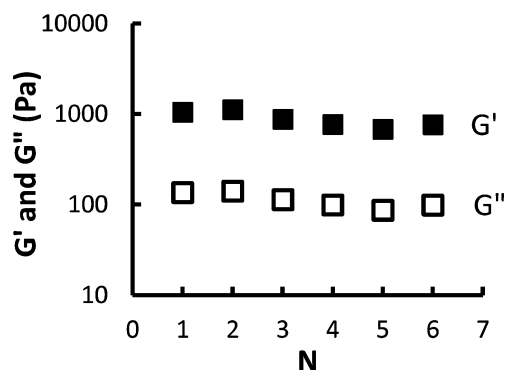
Figure 7. G' and G'' at a volume fraction of 0.87% as a function of the number of homogenization passes (N).

length of the microfibrils decreased and that shorter rodlike particles were formed when N increased, as described earlier in this letter. The presence of a fraction of significantly shorter rodlike particles will to first approximation decrease the volume fraction of long fibrils, which in turn decreased the elastic modulus G'. A more detailed study of the rheological behavior of CMF dispersions from BC will be presented in a follow-up paper.

CONCLUSIONS

We showed that a colloidal dispersion of fiberlike particles from bacterial cellulose can be prepared from commercial Nata de Coco pellicle sources using a high-energy deagglomeration process. The dispersions of CMF particles form colloidal gels at low concentrations. Confocal microscopy images showed that the distribution of microfibrils in these gels is very inhomogeneous. Because of their attractive nature, the CMFs form large inhomogeneous flocs, which are surrounded by a less-concentrated phase. The size of these flocs increased with CMF concentration while the size of the bundles stayed constant and the size of the voids decreased. The observed percolation threshold in BC dispersions is lower than the theoretical prediction, which is accounted for by the attractive interactions in the system. Rheological measurements confirmed the formation of gels and showed that the dispersions are very shear-thinning. We believe that colloidal dispersions of cellulose microfibrils from bacterial cellulose would form an interesting system for studying the relationships between the microstructure and the rheology of attractive, highly shape-anisotropic, semiflexible fiberlike colloidal particles.

ASSOCIATED CONTENT

Ⓢ Supporting Information
Calculation of van der Waals forces, additional CLSM images, and sedimentation profile of a low concentration CMF dispersion. This material is available free of charge via the Internet at http://pubs.acs.org

AUTHOR INFORMATION

Corresponding Authors
*E-mail: anke.kuijk@unilever.com.
*E-mail: krassimir.velikov@unilever.com.

■ REFERENCES

(1) Gabriel, J. C. P.; Davidson, P. New trends in colloidal liquid crystals based on mineral moieties. *Adv. Mater.* **2000**, *12*, 9−20.

(2) Lagerwall, J. P. F.; Scalia, G. A new era for liquid crystal research: applications of liquid crystals in soft matter nano-, bio- and microtechnology. *Curr. Appl. Phys.* **2012**, *12*, 1387−1412.

(3) Lieleg, O.; Schmoller, K. M.; Cyron, C. J.; Luan, Y. X.; Wall, W. A.; Bausch, A. R. Structural polymorphism in heterogeneous cytoskeletal networks. *Soft Matter* **2009**, *5*, 1796−1803.

(4) Lin, Y. C.; Koenderink, G. H.; MacKintosh, F. C.; Weitz, D. A. Control of non-linear elasticity in F-actin networks with microtubules. *Soft Matter* **2011**, *7*, 902−906.

(5) Okiyama, A.; Motoki, M.; Yamanaka, S. Bacterial cellulose IV. Application to processed foods. *Food Hydrocolloids* **1993**, *6*, 503−511.

(6) Kolakovic, R.; Peltonen, L.; Laaksonen, T.; Putkisto, K.; Laukkanen, A.; Hirvonen, J. Spray-dried cellulose nanofibers as novel tablet excipient. *AAPS PharmSciTech* **2011**, *12*, 1366−1373.

(7) Rodriguez, K.; Gatenholm, P.; Renneckar, S. Electrospinning cellulosic nanofibers for biomedical applications: structure and in vitro biocompatibility. *Cellulose* **2012**, *19*, 1583−1598.

(8) Evans, B. R.; O'Neill, H. M.; Malyvanh, V. P.; Lee, I.; Woodward, J. Palladium-bacterial cellulose membranes for fuel cells. *Biosens. Bioelectron.* **2003**, *18*, 917−923.

(9) Moon, R. J.; Martini, A.; Nairn, J.; Simonsen, J.; Youngblood, J. Cellulose nanomaterials review: structure, properties and nanocomposites. *Chem. Soc. Rev.* **2011**, *40*, 3941−3994.

(10) Yamamoto, H.; Horii, F. In situ crystallization of bacterial cellulose I. Influences of polymeric additives, stirring and temperature on the formation celluloses I_α and I_β as revealed by cross-polarization magic-angle-spinning (CP/MAS) ^{13}C NMR spectroscopy. *Cellulose* **1994**, *1*, 57−66.

(11) Tokoh, C.; Takabe, K.; Sugiyama, J.; Fujita, M. Cellulose synthesized by Acetobacter xylinum in the presence of plant cell wall polysaccharides. *Cellulose* **2002**, *9*, 65−74.

(12) Yamanaka, S.; Watanabe, K.; Kitamura, N.; Iguchi, M.; Mitsuhashi, S.; Nishi, Y.; Uryu, M. The structure and mechanical-properties of sheets prepared from bacterial cellulose. *J. Mater. Sci.* **1989**, *24*, 3141−3145.

(13) Nakagaito, A. N.; Iwamoto, S.; Yano, H. Bacterial cellulose: the ultimate nano-scalar cellulose morphology for the production of high-strength composites. *Appl. Phys. A* **2005**, *80*, 93−97.

(14) Eichhorn, S. J. Cellulose nanowhiskers: promising materials for advanced applications. *Soft Matter* **2011**, *7*, 303−315.

(15) Hubbe, M. A.; Rojas, O. J. Colloidal stability and aggregation of lignocellulosic materials in aqueous suspension: a review. *BioResources* **2008**, *3*, 1419−1491.

(16) Okiyama, A.; Motoki, M.; Yamanaka, S. Bacterial cellulose III. Development of a new form of cellulose. *Food Hydrocolloids* **1993**, *6*, 493−501.

(17) Sun, C. True density of microcrystalline cellulose. *J. Pharm. Sci.* **2005**, *94*, 2132−2134.

(18) Luengo Hendriks, C. L.; van Vliet, L. J. Morphological Scale-Space to Differentiate Microstructures of Food Products. *Proceedings 6th Annual Conference of the Advanced School for Computing and Imaging*, Lommel, Belgium, June 14−16, 2000;ASCI, Delft, 2000; pp 289−293.

(19) Kose, R.; Mitani, I.; Kasai, W.; Kondo, T. "Nanocellulose" as a single nanofiber prepared from pellicle secreted by gluconacetobacter xylinus using aqueous counter collision. *Biomacromolecules* **2011**, *12*, 716−720.

(20) Hobbie, E. K.; Fagan, J. A.; Obrzut, J.; Hudson, S. D. Microscale polymer-nanotube composites. *ACS Appl. Mater. Interfaces* **2009**, *1*, 1561−1566.

(21) Watanabe, K.; Tabuchi, M.; Morinaga, Y.; Yoshinaga, F. Structural features and properties of bacterial cellulose produced in agitated culture. *Cellulose* **1998**, *5*, 187−200.

(22) Lee, K.-Y.; Quero, F.; Blaker, J. J.; Hill, C. A. S.; Echhorn, S. J.; Bismarck, A. Surface only modification of bacterial cellulose nanofibres with organic acids. *Cellulose* **2011**, *18*, 595−605.

(23) Kim, C.; Liu, Y.; Kuhnle, A.; Hess, S.; Viereck, S.; Danner, T.; Mahadevan, L.; Weitz, D. A. Gravitational stability of suspensions of attractive colloidal particles *Phys. Rev. Lett.* **2007**, *99*.

(24) Hill, R. J. Elastic modulus of microfibrillar cellulose gels. *Biomacromolecules* **2008**, *9*, 2963−2966.

(25) Vigolo, B.; Coulon, C.; Maugey, M.; Zakri, C.; Poulin, P. An experimental approach to the percolation of sticky nanotubes. *Science* **2005**, *309*, 920−923.

(26) Kropholler, H. W.; Sampson, W. W. The effect of fibre length distribution on suspension crowding. *J. Pulp Pap. Sci.* **2001**, *27*, 301−305.

(27) Saarikoski, E.; Saarinen, T.; Samela, J.; Seppälä, J. Flocculated flow of microfibrillated cellulose water suspensions: an imaging approach for characterisation of rheological behaviour. *Cellulose* **2012**, *19*, 647−659.

(28) Pääkkö, M.; Ankerfors, M.; Kosonen, H.; Nykänen, A.; Ahola, S.; Osterberg, M.; Ruokolainen, J.; Laine, J.; Larsson, P. T.; Ikkala, O.; Lindström, T. Enzymatic hydrolysis combined with mechanical shearing and high-pressure homogenization for nanoscale cellulose fibrils and strong gels. *Biomacromolecules* **2007**, *8*, 1934−1941.